Mechanics of Materials 149 (2020) 103538

Contents lists available at ScienceDirect

Mechanics of Materials

journal homepage: www.elsevier.com/locate/mechmat

Research paper

Temperature effects on the mechanical properties of hybrid composites reinforced with vegetable and glass fibers

Camelia Cerbu[a], Huaiwen Wang[b,*], Marius Florin Botis[c], Zhen Huang[b], Costel Plescan[c]

[a] Department of Mechanical Engineering, Faculty of Mechanical Engineering, Transilvania University of Brasov, B-dul Eroilor, No. 29, Brasov 500036, Romania
[b] Tianjin Key Laboratory of Refrigeration Technology, Tianjin University of Commerce, No. 409 Guangrong Road, Beichen District, Tianjin 300134, PR China
[c] Department of Civil Engineering, Faculty of Civil Engineering, Transilvania University of Brasov, B-dul Eroilor, No. 29, Brasov 500036, Romania

ARTICLE INFO

Keywords:
Temperature
Composite materials
Flax fiber
Jute fiber
Glass fiber
Thermal stress
Tensile test
Thermogravimetric analysis

ABSTRACT

Although there are numerous applications for composite materials reinforced with vegetable textile fibers in outdoor parts and components (e.g., acoustic or thermal insulation panels in construction, furniture for gardens), only a few studies have reported the effects of temperature on hybrid composites reinforced with both glass and vegetable fibers. The main goal of this study was to analyze the effects of temperature on the tensile properties of five types of polymeric composites with different reinforcements: jute fabric, glass and jute fabric, flax fabric, glass and flax fabric, and glass fabric. Our method consisted of tensile testing all five types of composites at room temperature (20 °C) and other different temperatures (50 °C and 70 °C). The greatest values of reduction in tensile strength were recorded for hybrid composites. Reductions of 42.3% and 49.6% at 50 °C and 70 °C, respectively, were observed for the composite reinforced with flax and glass fibers. Reductions of 34.6% and 60% at 50 °C and 70 °C, respectively, were observed for the composite reinforced with jute and glass fibers. Finite element analysis of representative volume elements was conducted to compute the residual thermal stresses developed in the fibers and in the matrices at interfaces. It was determined that the thermal stresses cause micro-cracks at the interfaces. Thermogravimetric analysis and microscopic analysis were also conducted to identify the causes of the significant decreases in tensile properties. The effects of the anisotropy of flax and jute fibers on the thermal stresses developed at fiber-matrix interfaces were analyzed as well.

1. Introduction

Currently, there is significant global interest regarding the use of the natural fibers as reinforcing materials in the industry of composite materials. The main goal is to replace classical reinforcing fibers (glass fibers, carbon fibers, boron fibers) in polymeric and non-polymeric resins with reinforcing fibers obtained from renewable and biodegradable materials, such as natural fibers. The main classes of natural fibers are vegetable textile fibers (flax, jute, hemp, sisal), wood fibers (oak, fir, walnut, spruce, beech fibers), and agricultural waste fibers (stems, leaves, walnut shells, corn cobs, banana peels). Polymeric composite materials reinforced with natural fibers are eco-friendly products with numerous applications including indoor and outdoor furniture, and construction elements (acoustic and thermal insulation panels for design, roof tiles, pavers that dampen shock) (Ramesh, 2019, Singh et al., 2018).

The main advantage of natural fibers is their lower density than the classical reinforcement fibers, which leads to a reduction in weight. It is also known that composite materials reinforced with natural fibers are advantageous for acoustic and thermal insulation (Cerbu, 2015, Cerbu and Cosereanu, 2016). However, there are some disadvantages of natural fibers, including greater moisture absorption in humid environments, which degrades mechanical properties, significant smoke generation when the composites burn, and degraded mechanical properties under long-term exposure to ultraviolet rays (Cerbu, 2015, Yan et al., 2015).

Based on modern industrial trends regarding the design of new products based on composite materials reinforced with natural fibers, many articles have been published in recent years on the analysis of the physical and mechanical properties of polymeric composites reinforced with flax or jute fibers (Cerbu, 2015, Cerbu, 2015, Cerbu and Cosereanu, 2016, Xu et al., 2019).

Replacing glass fibers with natural fibers leads to the degradation of mechanical properties (tensile strength, Young's modulus, bending strength, and modulus of elasticity during bending), while the weight of a composite is reduced (Cerbu, 2017, Xu et al., 2019). In most cases,

* Corresponding author.
E-mail address: wanghw@tjcu.edu.cn (H. Wang).

https://doi.org/10.1016/j.mechmat.2020.103538
Received 5 August 2019; Received in revised form 12 July 2020; Accepted 13 July 2020
Available online 15 July 2020

Table 1
Coefficients of thermal expansion corresponding to the reinforcement fibers, epoxy resins, and composite materials reinforced with vegetable fibers

Material		Thermal expansion coefficient ($\times 10^{-6}$/°C) Longitudinal direction of the fiber α_{1f}	Transverse direction of the fiber α_{2f}	Source
Fibers:				
E-glass fiber		5.4	5.4	(Properties of E-glass fibres, 2019, Sathishkumar et al., 2014, Thomason et al., 2017)
Carbon		−0.4	18	(Thomason et al., 2017)
Aramid		3.6	77	(Thomason et al., 2017)
Jute	(at 25 °C)	−0.6	77.2	(Cichocki and Thomason, 2002)
	(at 50 °C)	−16	121.6	
	(at 75 °C)	−24.8	-	
Flax	(at 25 °C)	−8.0	82.7•	(Thomason et al., 2017)
	(at 50 °C)	−6.9	65.2	
Sisal	(at 25 °C)	−3.9	79.0	
	(at 50 °C)	−4.0	76.8	
Epoxy resins:				
Epolam 2035 epoxy		62		(Technical Data Sheet, 2019)
Epolam 2031 epoxy		80		(Technical Data Sheet, 2019)
D.E.R.™ 332 epoxy		140	(Saidina et al., 2007)	
Composite materials reinforced with vegetable fiber fabrics:				
Jute / Crystic P990 polyester resin	80	(Safiee et al., 2011)		

only a portion of the layers in a composite, typically core layers, are reinforced with vegetable textile fibers, while the shell layers are still reinforced with glass fibers, particularly for parts subjected to bending. Therefore, it is important to analyze the mechanical properties of hybrid polymeric composite materials reinforced with both glass and vegetable textile fibers (Cerbu, 2017, Xu et al., 2019).

Many articles have focused on the effects of technology and different surface treatments that are applied to vegetable fibers prior to manufacturing composite materials to improve interfacing between vegetable fibers and resin to improve the strength and stiffness of composites (Ramesh, 2019, Singh et al., 2018, Pitarresi et al., 2015). Stiffness hardening has been observed after a few quasi-static loading-unloading cycles accompanied by hysteresis based on the viscoelastic behavior of flax fibers (Pitarresi et al., 2015).

Additionally, it has been demonstrated that higher temperatures accelerate the aging process of jute-fiber-reinforced polymer composites during immersion in water and alkali solutions. The aging process during 45 days of immersion in water at 40 °C reduces the tensile strength and the modulus of elasticity by 22.5% and 19%, respectively (Ma et al., 2018).

In contrast, exposing jute epoxy composite specimens to liquid nitrogen for 5 h to reduce the specimen temperature to −60°C leads to the enhancement of mechanical properties (compression strength, bending strength, and inter-laminar shear strength) (Prasob and Sasikumar, 2019).

A recent study (Habibi et al., 2019) on the fatigue behavior of nonwoven flax composites reported a pronounced decrease in the dynamic modulus during fatigue loading at 75 °C compared to the value at 23 °C.

The current state of research on hybrid composite materials reinforced with both inorganic fibers (glass, carbon) and vegetable textile fibers (flax, jute, *Pennisetum purpureum*) highlights the potential of such composites from different perspectives, such as strength, stiffness, and energy absorbed during impact loading (Al-Hajaj et al., 2019, Cerbu and Cosereanu, 2016, Ridzuan et al., 2019, Xu et al., 2019). Hybrid composites fabricated from epoxy resin with shell layers reinforced by woven carbon fibers and core layers reinforced by cross-ply flax fibers exhibited better impact properties (higher penetration energy, smaller damage areas) compared to similar hybrid composites with core layers reinforced by unidirectional flax fibers (Al-Hajaj et al., 2019).

The authors of (Ridzuan et al., 2019) reported that for a *Pennisetum purpureum*/glass-reinforced epoxy composite, stiffness decreases significantly with increasing temperature (40 °C, 60 °C, and 80 °C), which increases the absorbed energy during impact testing. Additionally, decreasing stiffness leads to increased peak deflection and extensive damage.

However, the literature generally lacks a focus on the influence of temperature on the mechanical properties of hybrid composite materials reinforced with both glass and vegetable textile fibers. Evaluating the effects of temperature on the mechanical properties of this type of hybrid composite is crucial based on their frequent use in outdoor applications (construction elements, furniture for gardens and terraces, door panels or subfloors for automobiles) (Cerbu, 2015, Ramesh, 2019, Singh et al., 2018).

The main goal of this study was to investigate the effects of two different temperatures (50 °C and 70 °C) on the mechanical properties of five types of fiber-reinforced epoxy composites (FRECs): (*i*) jute fabric, (*ii*) both glass and jute fabric, (*iii*) flax fabric, (*iv*) both glass and flax fabric, and (*v*) glass fabric. First, we comparatively analyzed the effects of temperature on the mechanical characteristics of these FRECs via tensile testing. Then, we used a micromechanical finite element model (FEM) to analyze the residual thermal stresses developed in both the fibers and epoxy matrix at fiber-matrix interfaces for three composite materials: epoxy resin reinforced with flax fibers, epoxy resin reinforced with jute fibers, and epoxy resin reinforced with glass fibers.

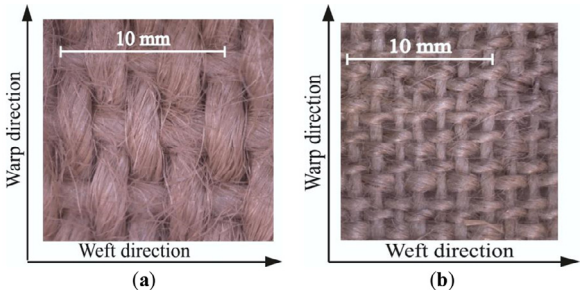

Fig. 1. Photos of fabrics made of vegetable fibers: (a) jute fabric and (b) flax fabric (Cerbu, 2015, Cerbu, 2017).

We then used thermogravimetric analysis (TGA) to analyze mass loss during heating to 800 °C for the reinforcement woven fabrics, epoxy resin, and composite materials tested. Finally, TGA and microscopic analysis of the samples were considered to explain the changes in tensile properties caused by increasing temperature.

The values of the thermal expansion coefficients corresponding to the reinforcement fibers (inorganic fibers and vegetable fibers) and to the epoxy resin are reported in Table 1. The anisotropy of the flax and jute fibers is reflected in their coefficients of thermal expansion.

2. Materials and methods

2.1. Materials tested

All the composite materials investigated in this study were based on Epolam 2015 epoxy resin reinforced with a bidirectional glass fabric and two types of plain-woven fabrics made of vegetable fibers (flax fibers, jute fibers).

Epolam 2015 epoxy resin (Axson) exhibits the following physical properties: viscosity of 1550 mPa•s, density of 1.15 g/ml, and mix ratio by weight of 32:100 between Epolam 2015 hardener and Epolam 2015 epoxy resin (Technical Data Sheet, 2019). The physical properties of the Epolam 2015 hardener are a viscosity of 70 mPa•s and a density of 0.95 g/ml. Following admixture of the Epolam 2015 hardener into the epoxy resin and hardening, the glass transition temperature is 88 °C, which limits the application of composite materials based on the Epolam 2015 epoxy-hardener system (Technical Data Sheet, 2019).

The glass woven fabric used in this study was Aeroglass, which has a weight per unit area of 200 g/m^2 and weave of 2 × 2 twill (Technical Data Sheet of glass fabric AEROGLASS 200 g/m2 twill, 2019). The glass yarn was EC9-136 for both the weft and warp directions of the woven fabric (Technical Data Sheet of glass fabric AEROGLASS 200 g/m2 twill, 2019).

Regarding the vegetable fiber fabrics, the density per unit area of jute flax fabric is 380 g/m^2 and its weave is a bidirectional plane with the same jute yarns in the weft and warp directions (Fig. 1a). Tudor (DINATEX S.R.L., Romania) flax fabric is a bidirectional fabric with a density of 280 g/m^2 and a plain weave (Fig. 1b). The weft yarn is thicker than the warp yarn in the case of the flax fabric, as shown in Fig. 1(b) and as defined in its technical data sheet (Data sheet of flax fabric Tudor, 2019).

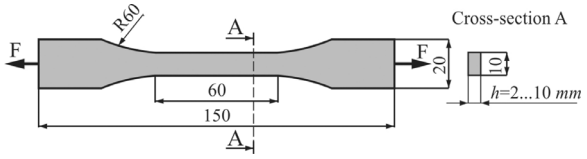

Fig. 2. Tensile specimen (EN ISO 527-4 1997).

2.2. Experimental methods

2.2.1. Sample preparation

The five types of composite materials listed in Table 2 were investigated in terms of their mechanical behavior during tensile testing under the action of heating at different temperatures (50 °C and 70 °C). The abbreviation codes used for the composite materials and the corresponding layer structures are also listed in Table 2. In Table 2, for the two hybrid composite materials (GJ-FREC and GF-FREC), their bottom and top shell layers were reinforced with glass fabric, while their core layers were reinforced with vegetable fibers (jute or flax fabric).

One panel with dimensions of 500 × 400 mm^2 was manufactured for each type of composite material using a hand layering technique that is suitable for Epolam 2015 epoxy resin (Technical Data Sheet, 2019). The fiber content was 40 wt% for each type of composite panel. The reinforcement fabrics were placed in the mold in a consistent orientation such that the warp direction of the fabric was parallel to the edge of the mold with a length of 500 mm. The composite panels were molded in the laboratory of the Mechanical Engineering Department of the Transilvania University of Brasov, Romania. The composite panels were stored for one week at room temperature (20 ± 1°C) prior to cutting the tensile specimens.

Tensile specimens were cut via milling using numerically controlled equipment. The dimensions and shape of the tensile specimens are presented in Fig. 2 in accordance with the European standard (EN ISO 527-4 1997) (EN ISO 527-4 1997). Because the flax yarns were different in thickness in the weft and warp directions of the flax fabric, two subsets of tensile specimens were cut parallel to the weft an warp directions for the composite materials reinforced with flax fabric (F-FREC and GF-FREC composites). We prepared five tensile specimens for each type of composite material, each direction of the reinforcing glass fabric (if appropriate according to Table 1), and each temperature for tensile testing (20 °C (room temperature), 50 °C, and 70 °C). The maximum test temperature was limited by the glass transition temperature (88 °C) corresponding to the Epolam 2015 epoxy-hardener system following polymerization (Technical Data Sheet, 2019). A total of 15 specimens were prepared for each composite material reinforced with jute or glass fabric alone (J-FREC, G-FREC, GJ-FREC) and 30 specimens were prepared for each of the composites reinforced with flax fabric (F-FREC and GF-FREC).

Table 2
Composite materials tested.

No.	Composite material	Abbreviation	Structure of the material	Direction
1	Jute-fiber-reinforced epoxy composite	J-FREC	- 4 layers made of epoxy reinforced with jute woven fabric.	-
2	Glass-and-jute-fiber-reinforced epoxy composite	GJ-FREC	- 1 bottom shell layer reinforced with glass fabric;- 2 core layers reinforced with jute fabric;- 1 top shell layer reinforced with glass fabric.	-
3	Flax-fiber-reinforced epoxy composite	F-FREC	- 8 layers reinforced with flax woven fabric.	Weft Warp
4	Glass-and-flax-fiber-reinforced epoxy composite	GF-FREC	- 2 bottom shell layers reinforced with glass fabric; - 4 core layers reinforced with flax fabric; - 2 top shell layers reinforced with glass fabric.	Weft Warp
5	Glass-fiber-reinforced epoxy composite	G-FREC	- 8 layers made of epoxy reinforced with glass woven fabric.	-

Fig. 3. Equipment used in this study.

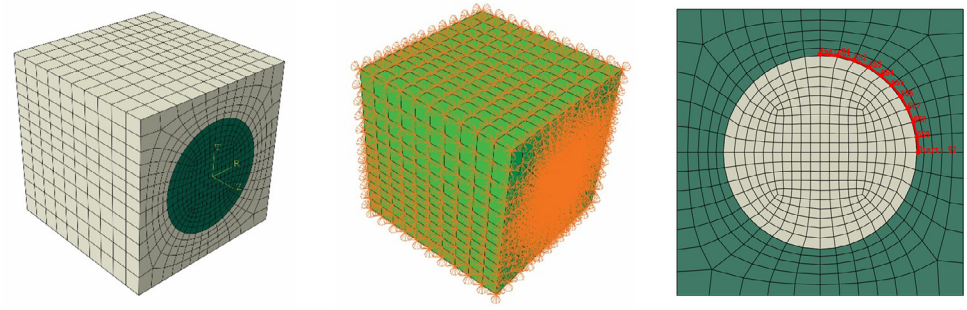

Fig. 4. FEM of a cubic RVE used to analyze the residual thermal stresses developed at interfaces: (a) FEM and cylindrical coordinate system, (b) boundary conditions, and (c) path of nodes defined in the square RVE for reporting residual thermal stress development.

Table 3
Elastic properties of the fibers and epoxy resin.

Material	Temperature	Elastic property					References
		E_{1f} (GPa)	E_{2f} (GPa)	G_{12f} (GPa)	ν_{12f}	ν_{21f}	
E-glass fiber	(at 25 °C)	72.4	-			0.22	(Properties of E-glass fibres, 2019, Sathishkumar et al., 2014, Laine et al., 2013)
Jute fiber	(at 0 °C)	40.3	6.6	4.7	0.14	0.02	(Singh et al., 2018, Cichocki and Thomason, 2002)
	(at 25 °C)	39.4	5.5	3.5	0.11	0.01	
	(at 50 °C)	38.9	3.8	3.3	0.08	0.01	
	(at 75 °C)	38.6	-	-	-	-	
Flax fiber	(at 0 °C)	65.7	1.1	1.5	0.4	-	(Ramesh, 2019, Thomason et al., 2017)
	(at 25 °C)	62.5	1.0	1.4	-	-	
	(at 50 °C)	60.2	0.75	1.1	-	-	
Epolam epoxy resin	(at 25 °C)	3.0	-			0.35	(Technical Data Sheet, 2019, Laine et al., 2013)

Table 4
Fiber contents and densities of Epolam 2015 epoxy resin composites.

No.	Composite material model	Fiber density (g/cm^3)	Epoxy density (g/cm^3)	Hardener density (g/cm^3)	Fiber mass ratio m_f (%)	Fiber volume ratio V_f (%)	References*
1	E-glass/epoxy	2.58	1.15**	0.95**	40	22.05	(Sathishkumar et al., 2014)
2	Jute fiber/epoxy	1.30				35.96	(Singh et al., 2018)
3	Flax fiber/epoxy	1.50				32.73	(Ramesh, 2019)

Note:
* References for fiber density.
** Densities in accordance with (Technical Data Sheet, 2019).

2.2.2. Tensile testing under temperature variation

Control tensile testing specimens were subjected to tensile testing at room temperature (approximately 20 °C). Tensile tests were conducted using an AG-IC 50 (SHIMADZU, Kyoto, Japan) tensile testing machine with digital controls and a maximum force of 50 KN.

Prior to the tensile tests at different temperatures (50 °C and 70 °C), the tensile specimens were preconditioned for 2 h at a humidity of 60% and temperature of 50 °C or 70 °C using a TEMI2500 (Hung TA INSTRUMENT CO. LTD., Taiwan, China) programmable temperature and humidity controller, as shown in Fig. 3(a). Conditioning of the specimens at the test temperatures prior to tensile testing was essential to ensure an uniform distribution of temperature throughout each specimen. The programmable temperature controller was located near the AG-IC 50 tensile testing machine in the laboratory.

An HT-8045A (Hung TA INSTRUMENT CO. LTD., Taiwan, China) high-temperature chamber fixed on the AG-IC 50 tensile testing

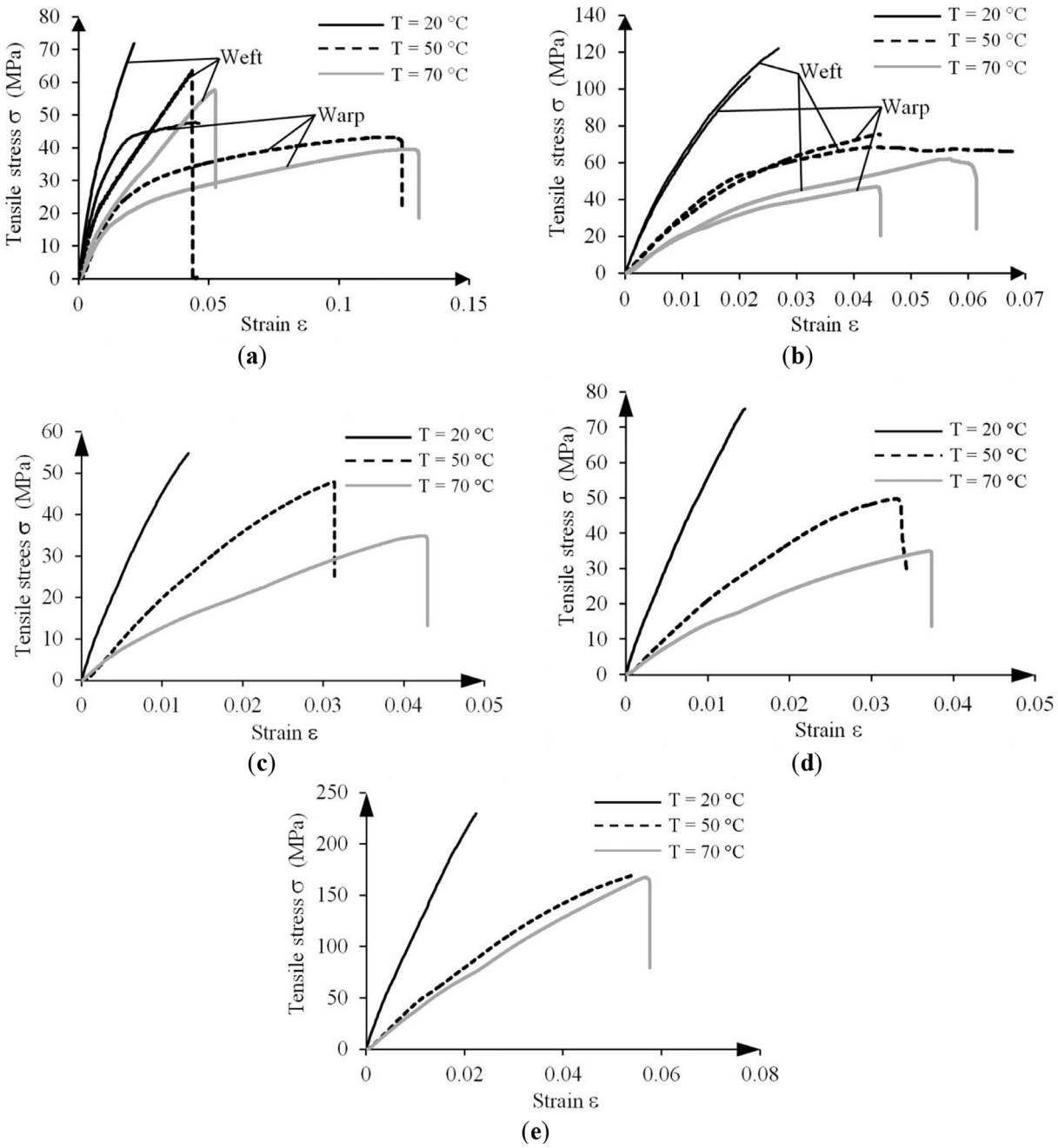

Fig. 5. Stress–strain curves recorded during tensile testing: (a) F-FREC composite, (b) GF-FREC composite, (c) J-FREC composite, (d) GJ-FREC composite, and (e) G-FREC composite.

machine (Fig. 3b) was used to analyze the effects of temperature at 50 °C and 70 °C. In Fig. 3(c), one can see a tensile specimen fabricated from the J-FREC composite clamped in the jaws of the tensile testing machine inside the high-temperature chamber.

(a) High-temperature chamber (HT-8045A), (b) tensile testing machine (AG-IC; 50 kN with programmable temperature and humidity controller (TEMI2500)), and (c) tensile specimen fabricated from the J-FREC composite during tensile testing at 50 °C or 70 °C inside the high-temperature chamber.

The dimensions of the cross sections of each tensile specimen were accurately measured with a precision of 0.1 mm and the results were used as input data for a software program at the beginning of each test. The loading speed was 1.5 mm/min for all tensile tests in accordance with the aforementioned standard (EN ISO 527-4 1997). The tensile testing machine allowed us to record the tensile force and elongation of the specimens over time. The experimental data were statistically processed to derive tensile σ-ε curves and mechanical properties, including the Young's modulus E and tensile strength (tensile stress corresponding to the maximum tensile force). The Young's modulus E was determinate on the linear portion of the σ-ε curves.

Finally, average values corresponding to both the moduli of elasticity and tensile strengths recorded during tensile tests at different temperatures (20 °C, 50 °C, 70 °C) were compared to analyze the effects of testing temperature and the type of reinforcement on mechanical characteristics.

2.2.3. TGA

A Shimadzu DTG-60 thermogravimetric analyzer was used to perform TGA. TGA was used to determine the variation in the mass of the specimens with temperature as the temperature increased continuously.

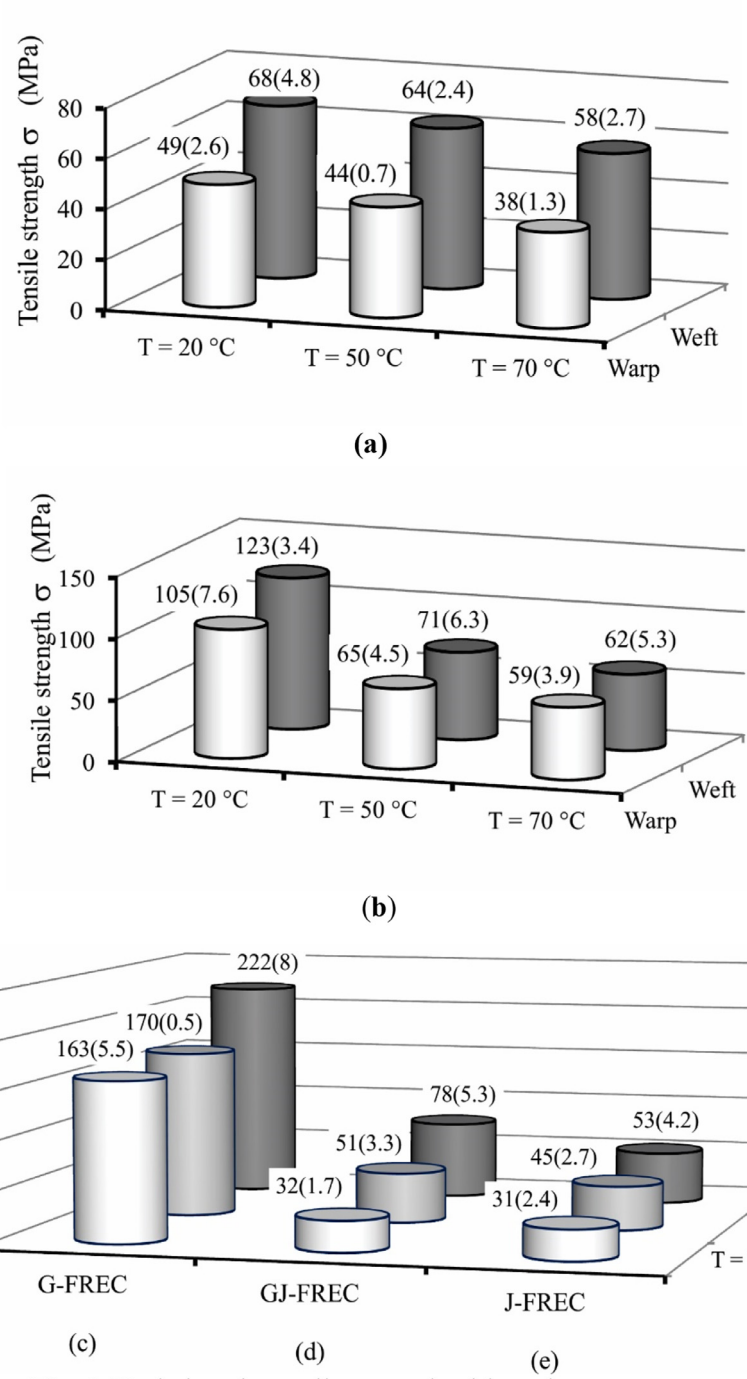

Fig. 6. Variations in tensile strength with testing temperature. (a) F-FREC composite, (b) GF-FREC composite, (c) G-FREC composite, (d) GJ-FREC, and (e) J-FREC. Note: all values are shown as x(y), where "x" indicates average values and "y" indicates standard deviation values.

TGA was performed on the following materials: jute fabric, flax fabric, pure Epolam 2015 epoxy resin hardened by adding Epolam 2015 hardener (32 wt%) (Technical Data Sheet, 2019), J-FREC composite, F-FREC composite, and G-FREC composite. The main purpose of this test was to determine the temperature at which mass loss began for each type of material. Samples with a mass of approximately 8 mg were prepared for each type of material. Testing consisted of heating each specimen to 800 ˚C at a rate of 20 ˚C /min in a nitrogen atmosphere with a flow rate of 30 ml/min.

2.2.4. Analysis of thermal stresses

In the literature, various types of models have been used for micromechanical analysis of the interactions between fibers and matrices in composite materials with a focus on the array arrangement of fibers (square array, hexagonal array) and shape of representative volume elements (RVEs) (Choi and Sankar, 2006, Kumar and Singh, 1995). In this research, square RVEs were used to analyze the residual thermal stresses developed at the interfaces between fibers and matrices. The square RVEs discussed in the literature are actually cubic RVEs and stresses are reported for middle square perpendicular cross sections (Kumar and Singh, 1995). The FEM corresponding to the geometry of a cubic RVE is presented in Fig. 4(a) in accordance with the procedure described in (Kumar and Singh, 1995). Finite element analysis was conducted using the Abaqus software. Both the fiber and

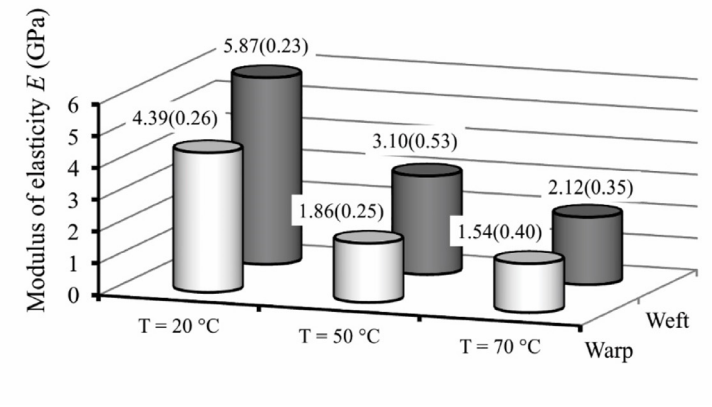

(a)

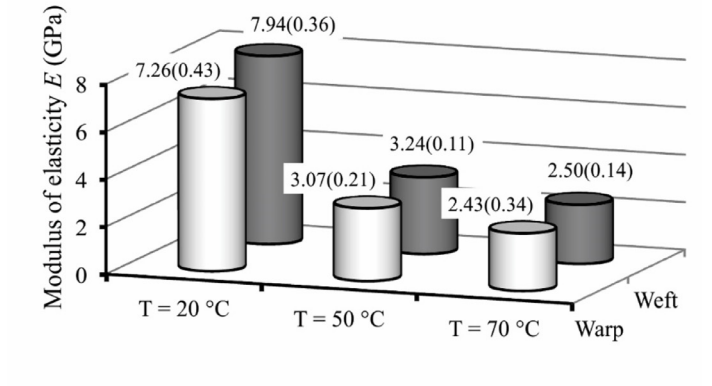

(b)

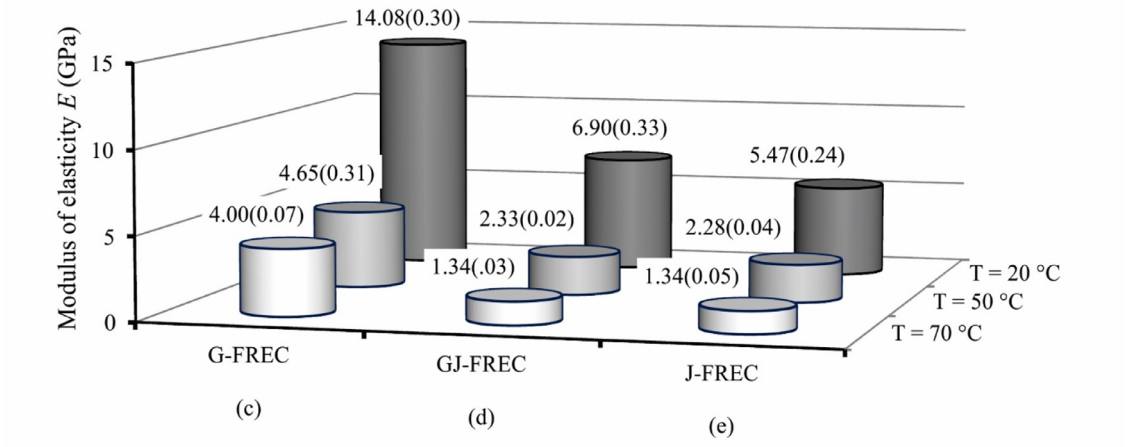

(c) (d) (e)

Fig. 7. Variations in the Young's modulus E with testing temperature:
(a) F-FREC composite, (b) GF-FREC composite, (c) G-FREC composite, (d) GJ-FREC, and (e) J-FREC.
Note: all values are shown as x(y), where "x" indicates average values and "y" indicates standard deviation values.

matrix regions are meshed by brick finite elements with eight nodes. An FEM consists of 3000 elements corresponding to the fiber region and 2040 elements corresponding to the matrix region.

Regarding boundary conditions, it is assumed that all nodes located on the boundary faces of the cubic RVE can move only along the direction perpendicular to the respective boundary face (Fig. 4b) in accordance with the procedure described in (Kumar and Singh, 1995). The effects of heating on the thermal stress development in a cubic RVE were analyzed. The initial temperature was 20°C for the FEM and the final temperature was either 50 °C or 70 °C.

The path of nodes highlighted in Fig. 4(c) is used to report the residual thermal stress development in both fibers and matrices at their interfaces. The order of the path of nodes follows the counterclockwise direction from 0° to 90°. The path of nodes is defined in a square middle cross section of the cubic RVE that is perpendicular to the fibers. Hereafter, this cross-section is referred to as a square RVE. The distributions of residual thermal stresses are plotted using a cylindrical coordinate system shown in Fig. 4(a). The origin of the cylindrical coordinate system is located at the center of the circular cross section of the fiber. This means that the radial direction of the coordinate system is the same as the radial direction of the fiber and the tangential direction is perpendicular to the fiber radius.

The main objective of our micromechanical analysis was to determine the effects of the anisotropy of the vegetable fibers (flax fibers and jute fibers) on the residual thermal stresses developed at the interfaces between these types of vegetable fibers and epoxy matrices.

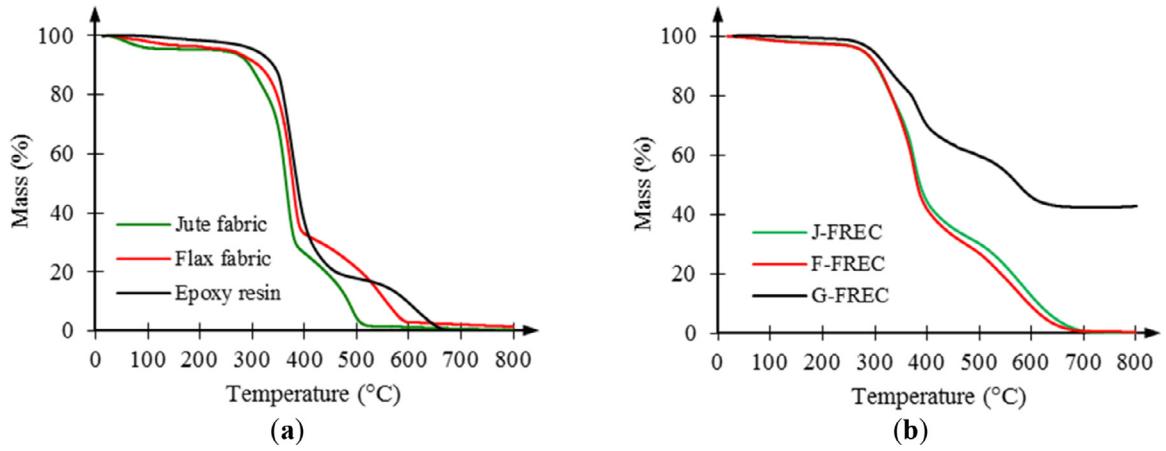

Fig. 8. TGA curves recorded for (a) vegetable woven fabrics used as reinforcement and Epolam 2015 epoxy resin, and (b) composite samples.

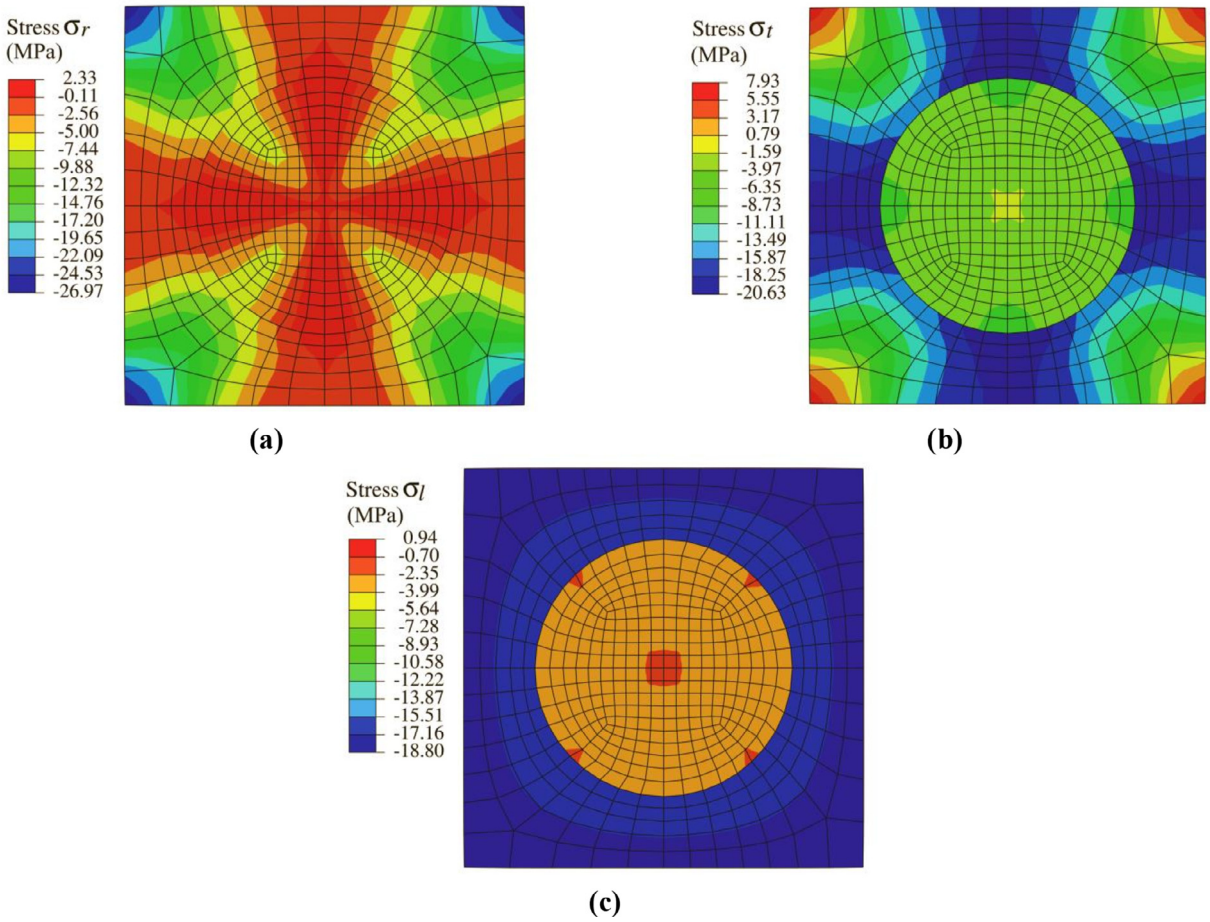

Fig. 9. Stresses developed over a square RVE for epoxy reinforced with flax fiber at $T = 70$ °C:
(a) radial thermal stresses σ_r, (b) tangential thermal stresses σ_t, and (c) longitudinal thermal stresses σ_l in the fiber direction.

The flax and jute fibers are anisotropic in terms of both their thermal expansion coefficients (Table 1) and elastic properties (Table 3). Furthermore, the thermal expansion coefficients corresponding to the flax and jute fibers are negative values along the longitudinal direction of these types of fibers. In a FEM of a cubic RVE, the elastic properties and thermal expansion coefficients corresponding to the flax or jute fibers are defined with respect to the cylindrical coordinate system shown in Fig. 4(a).

Glass fibers are isotropic in terms of their thermomechanical properties (Tables 1 and 3). The thermal expansion of the glass fibers is much lower than that of the epoxy resin used in this study (Table 1).

Three different models of a cubic RVE were considered depending on the combination of fibers and matrices, namely an epoxy matrix reinforced with flax fiber, epoxy matrix reinforced with jute fiber, and epoxy matrix reinforced with glass fiber. The fiber volume fraction corresponding to each model is listed in the final column of Table 4. The fiber volume fractions were computed based on a fiber mass ratio of 40 wt%, which was used for all composites considered in this study (see Section 2.2.1), and based on the density values corresponding to the fibers and epoxy resin, which are listed in Table 4.

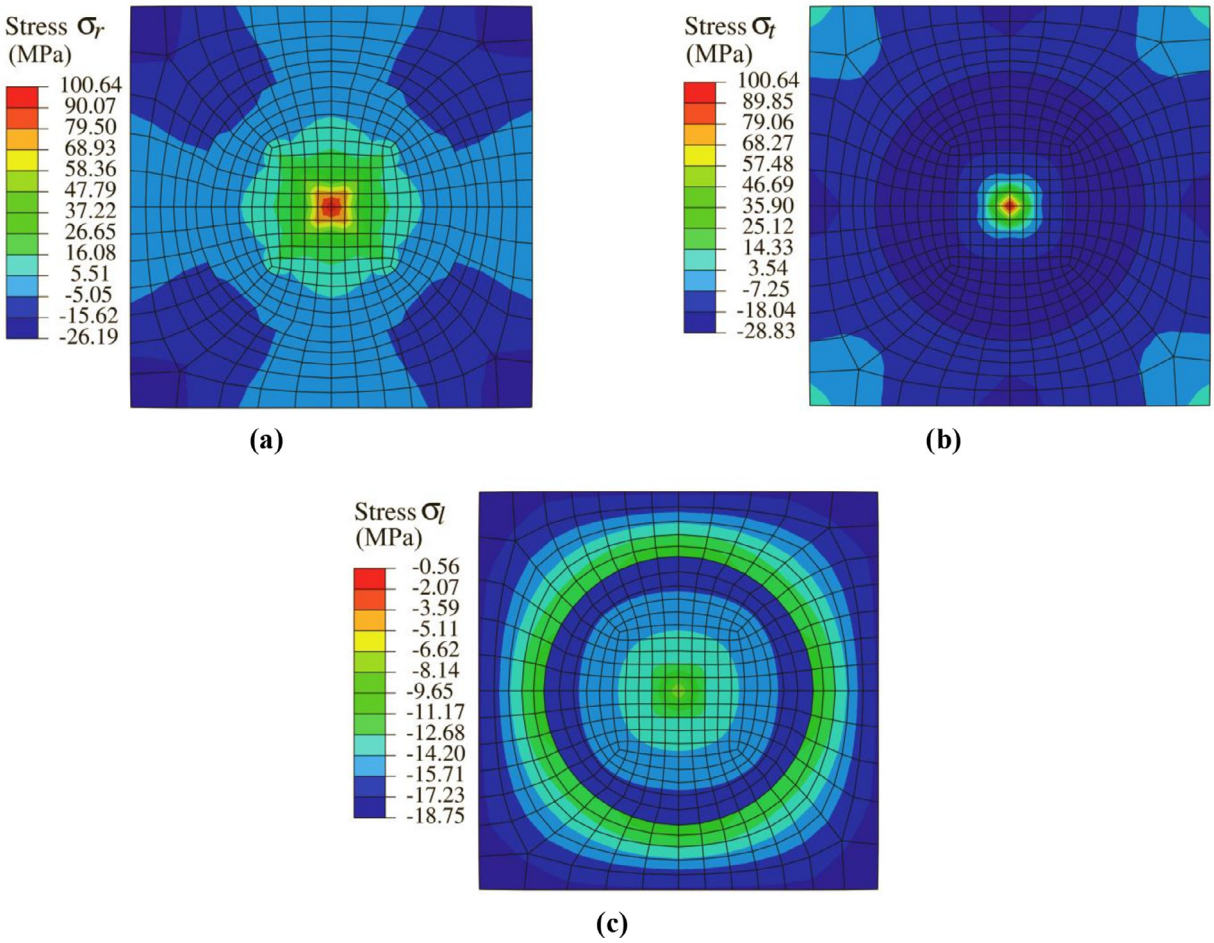

Fig. 10. Stresses developed over a square RVE for epoxy reinforced with jute fiber at $T = 70$ °C: (a) radial thermal stresses σ_r, (b) tangential thermal stresses σ_t, and (c) longitudinal thermal stresses σ_l in the fiber direction.

The residual thermal stresses derived via micromechanical analysis can be used to explain the effects of temperature changes on the tensile properties of the composite materials considered in this study. Specifically, we analyzed the residual thermal stresses developed in the radial and tangential directions of fiber-matrix interfaces for both fibers and epoxy matrices based on the three different FEMs.

2.2.5. Microscopic analysis

A Keyence-VHX600 (Japan) digital microscope was used to observe the changes in tensile properties that occurred during tensile testing at elevated temperatures. Micro-cracks in the matrices (epoxy resin) and changes at the interfaces between matrices and reinforcement fibers (glass, flax, and jute fibers) were observed.

3. Results

3.1. Results of tensile testing

The mean σ-ε curves recorded for each type of composite material are presented in Fig. 5 for all test temperatures (20 °C, 50 °C, and 70 °C). It is noteworthy that in the case of the control specimens tested at room temperature (20 °C), the σ-ε curves were recorded by the tensile testing machine until the maximum tensile force was reached (Fig. 5).

One can see that the initial slope of the σ-ε curve decreases as the test temperature increases. This indicates that the Young's modulus E decreases as the test temperature increases. The maximum tensile stress also decreases as temperature increases (Fig. 5).

The variations in tensile strength with test temperature are plotted in Fig. 6 for all of the composite materials tested.

In the case of the F-FREC composite, it is visible that the tensile strength is 5.9% lower and 14.7% lower at 50 °C and 70 °C, respectively, compared to the value recorded at 20 °C, when the tensile force is parallel to the weft direction of the flax fabric. The reductions in tensile strength are 10.2% and 22.5% at 50 °C and 70 °C, respectively, when tensile loading is applied in the warp direction for the F-FREC composite (Fig. 6a).

The reductions in tensile strength are much greater for the GF-FREC hybrid composite with values of 42.3% and 49.6% at 50 °C and 70 °C, respectively, in the weft direction, and 38.1% and 43.8% at 50 °C and 70 °C, respectively, in the warp direction (Fig. 6b).

In the case of the G-FREC composite, the tensile strength is 23.4% lower and 26.6% lower at 50 °C and 70 °C, respectively, compared to the value recorded during tensile testing at 20 °C (Fig. 6c).

The tensile strength is 15.1% lower and 41.5% lower at 50 °C and 70 °C, respectively, for the J-FREC composite (Fig. 6e). In the case of the GJ-FREC hybrid composite, significant degradation of tensile strength can be observed with values 34.6% lower and 60% lower at 50 °C and 70 °C, respectively (Fig. 6d).

The variation in the Young's modulus E with testing temperature is plotted in Fig. 7 for all of the tested composite materials.

In the case of the F-FREC composite subjected to tensile testing in the weft direction of the flax fabric, the Young's modulus E decreases relative to the values recorded for the control specimens with reductions of 47.2% and 63.8% at 50 °C and 70 °C, respectively (Fig. 7a). Similar reductions are recorded for the case of tensile loading in the warp direction with values of 57.6% and 64.8% at 50 °C and 70 °C,

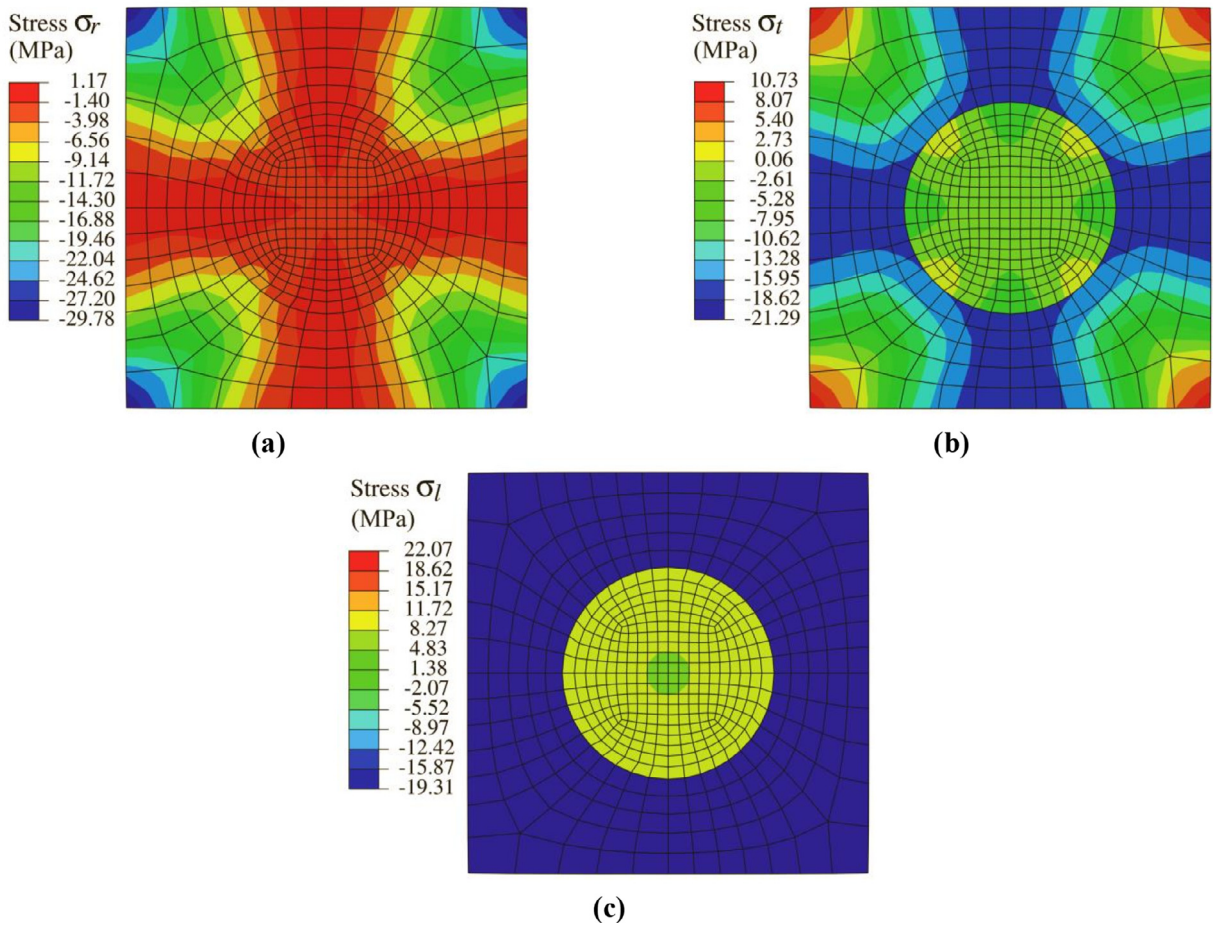

Fig. 11. Stresses developed over a square RVE for epoxy reinforced with glass fiber at $T = 70$ °C: (a) radial thermal stresses σ_r, (b) tangential thermal stresses σ_t, and (c) longitudinal thermal stresses σ_l in the fiber direction.

respectively (Fig. 7a).

In the case of the GF-FREC hybrid composite, in contrast to the results for tensile strength, the Young's modulus E reductions are similar to those of the F-FREC composite with values of 59.2% and 68.6% at 50 °C and 70 °C, respectively, in the weft direction of the flax fabric, and 57.8% and 66.6% at 50 °C and 70 °C, respectively, in the warp direction of the flax fabric.

In the case of the G-FREC composite, the modulus of elasticity is 67% lower and 71.6% lower at 50 °C and 70 °C, respectively, compared to the value recorded at 20 °C (Fig. 7c).

The modulus of elasticity is 58.2% lower and 75.5% lower at 50 °C and 70 °C, respectively, compared to the value recorded at 20 °C for the J-FREC composite (Fig. 7e). Similar reductions in the modulus of elasticity were recorded in the case of the GJ-FREC hybrid composite with values of 66.3% and 79.7% at 50 °C and 70 °C, respectively (Fig. 7d).

3.2. Results of TGA

The mass losses recorded in the case of the jute fabric are 1.5% at 50 °C, 3% at 70 °C, 30% at 348 °C, and 99.7% at 800 °C (Fig. 8a). In the case of the flax fabric, the recorded mass losses are 0.5% at 50 °C, 1.2% at 70 °C, 35% at 366 °C, and 98.5% at 800 °C (Fig. 8a). The small values of mass loss up to 70 °C can be attributed to the drying of the samples in both cases.

The epoxy Epolam 2015 resin is more stable than the natural fibers with no mass loss up to 90 °C and recorded mass loss values of 21% at 360 °C, 80% at 460 °C, and 98.8% at 680 °C (Fig. 8a).

The thermogravimetric stability of composite materials reinforced with jute or flax fabrics is improved by the good stability of the epoxy resin (Fig. 8b). For the J-FREC composite, the mass loss values are 0.34% at 50 °C, 0.85% at 70 °C, 70% at 357 °C, and 99.8% at 741 °C (Fig. 8b). Superior stability of the F-FREC composite was observed compared to the flax fabric with mass loss values of 0.5% at 50 °C, 0.85% at 70 °C, 35% at 362 °C, and 99.5% at 800 °C (Fig. 8a).

The best thermogravimetric stability was recorded for the G-FREC composite with no mass loss until 110 °C and recorded mass loss values of 18% at 360 °C, 38% at 460 °C, and 57.1% at 800 °C (Fig. 8b). This is because the melting point of the E-glass fibers is 846 °C (Technical Data Sheet, 2019).

3.3. Residual thermal stresses

Residual thermal stresses were analyzed for square RVE cross sections perpendicular to the fibers in each sample. The distributions of the thermal stresses in the radial, tangential, and longitudinal directions are presented in Figs. 9–11 for FEMs corresponding to different fiber-matrix combinations. All residual thermal stresses are reported in the cylindrical coordinate system described in Fig. 4(a).

The distributions of the residual thermal stresses on the path of nodes highlighted in Fig. 4(c), which are located at the interface between flax fibers and the epoxy matrix, are presented in Fig. 12 for the cases of heating from 20 °C to 50 °C and from 20 °C to 70 °C.

The distributions of the residual thermal stresses at the interfaces between jute fibers and the epoxy matrix are plotted in Fig. 13. Fig. 14 presents the distribution of residual thermal stresses at the interfaces

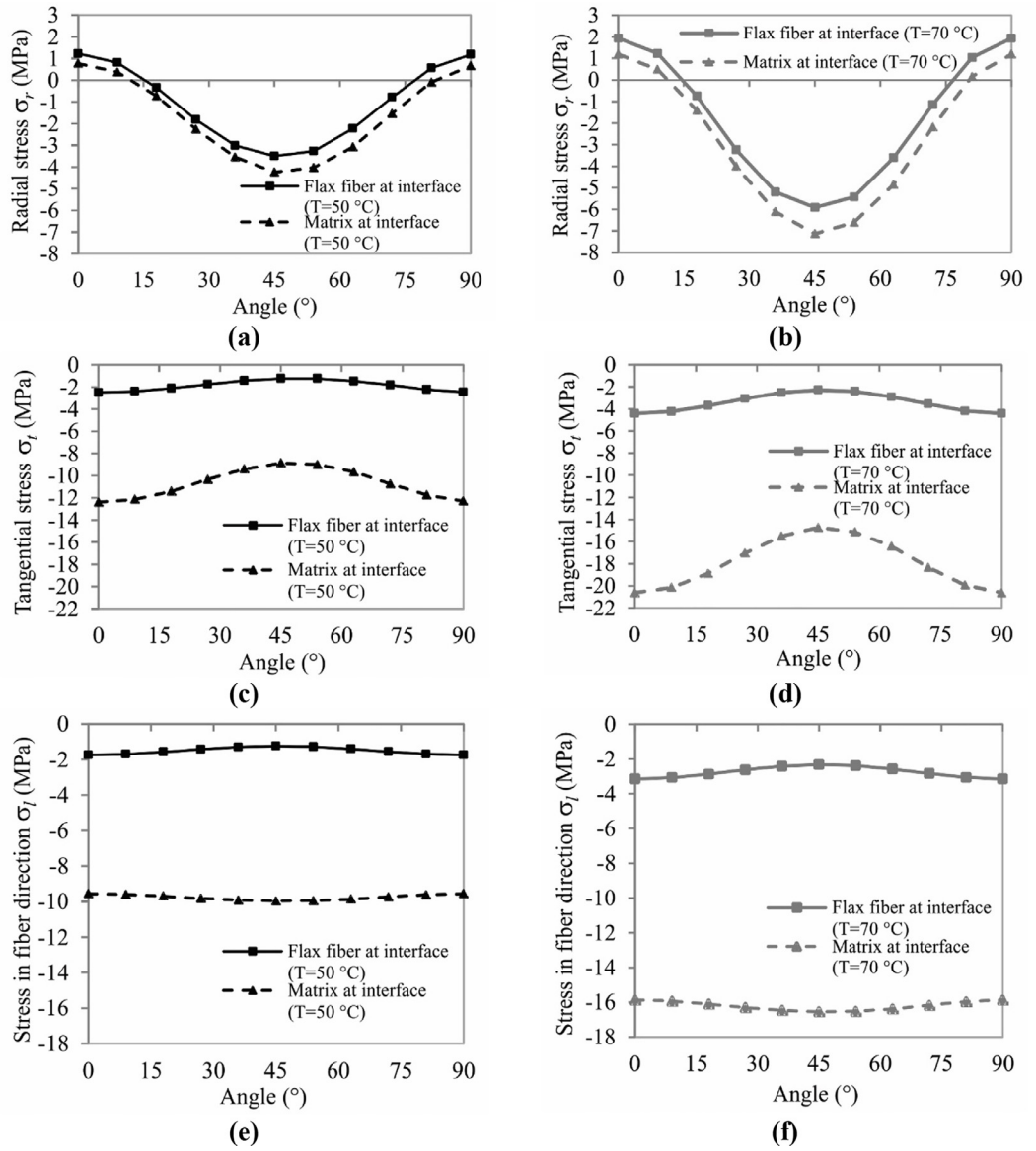

Fig. 12. Distribution of residual thermal stresses at the interface between flax fibers and the epoxy matrix after heating to $T = 50$ °C or $T = 70$ °C: (a, b) radial stresses σ_r, (c, d) tangential stresses σ_t, and (e, f) longitudinal stresses σ_l in the fiber direction.

between glass fibers and the epoxy matrix.

Based on Figs. 12–14, one can conclude that the maximum values of the radial thermal stresses correspond to the direction defined by a 45° angle for all types of FEMs analyzed. The maximum values of the tangential thermal stress correspond to the directions defined by angles of 0° and 90°. The maximum values of the longitudinal thermal stresses developed in the fibers of all FEMs also correspond to the directions defined by angles of 0° and 90°. However, the longitudinal thermal stresses developed in the glass fibers at the interface are positive, while the longitudinal thermal stresses developed in the flax and jute fibers at the interface are negative. This is because the thermal expansion coefficients corresponding to the fiber direction are negative for the two types of vegetable fibers (Table 1). The maximum values of the longitudinal thermal stresses developed in the epoxy resin for all FEMs correspond to the directions defined by a 45°- angle.

The residual thermal stresses developed in the fibers differ from those developed in the epoxy matrix for the nodes located at the fiber-matrix interfaces in all three types of FEMs analyzed. The greatest difference between the radial stresses developed in the fibers and the radial stresses developed in the epoxy matrix at the interfaces corresponds to the node located at the midpoint of the path highlighted in Fig. 4(c), which corresponds to a 45°-angle (Figs. 12a–14a).

The values of the residual tangential stresses developed in the fibers at the fiber-matrix interfaces vary significantly with the tangential stresses developed in the epoxy matrix at the interfaces (Fig. 12b–14b). The same phenomenon was observed for the residual thermal stresses developed in the fiber direction.

In summary, different thermal stresses developed in the fibers compared to the matrix and the magnitude of the interface stresses correspond to the development of micro-cracks at the interfaces between fibers and the matrix.

3.4. Damaged areas in specimens

Photos of the tensile specimens, which were acquired using an electronic microscope, are presented in Figs. 15 to 17 to highlight micro-crack development at the interface areas between the reinforcing fibers and epoxy matrix after heating the specimens from 20 °C to 70 °C. Fig. 15(a) presents a microscopic photo of the cross section of a specimen made from the F-FREC composite after heating to 70 °C. Areas A

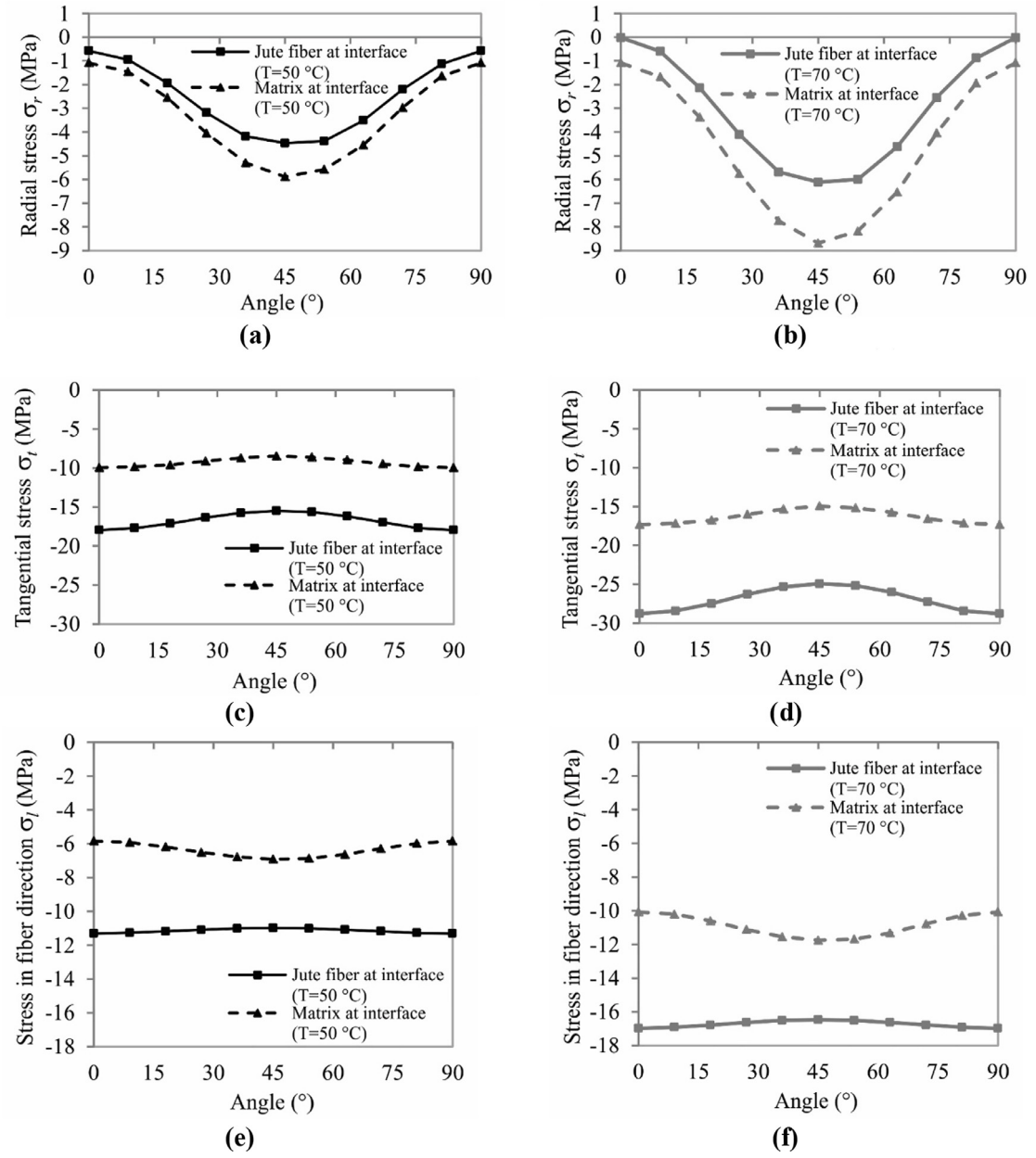

Fig. 13. Distribution of residual thermal stresses at the interface between jute fibers and the epoxy matrix after heating to $T = 50$ °C or $T = 70$ °C: (a, b) radial stresses σ_r, (c, d) tangential stresses σ_t, and (e, f) longitudinal stresses σ_l in the fiber direction.

and B are presented at an increased scale (lens: X 250) in Figs. 15(b) and 15(c), respectively, to highlight the detachments of flax fibers from the epoxy matrix.

Fig. 16(a) presents a microscopic photo of a specimen made from the GF-FREC hybrid composite to highlight the detachments of flax fibers from the epoxy matrix (Fig. 16b) in the layers reinforced with flax fabric and the detachments of glass fibers from the epoxy matrix (Fig. 16c) in layers reinforced with glass fabric. The photo of the GF-FREC composite contains three distinct areas: a core layer reinforced with flax fabric, and top and bottom shell layers reinforced with glass fabric (Fig. 16a). Inter-laminar micro-cracks are also highlighted at the interface between the core layers reinforced with flax fabric and shell layers reinforced with glass fabric (Fig. 16c). These cracks are attributed to the different thermal expansion coefficients of the two types of layers based on different reinforcing fibers.

Detachment of jute fibers from the epoxy resin can also be observed in the layers of the J-FREC composite (Fig. 17a). In Fig. 17(b), some areas exhibit detachment of glass fibers from the epoxy resin for the G-FREC composite material.

4. Discussion

The results reported for TGA led to the conclusion that all composite materials considered in this study are stable up to 70 °C and that mass loss is not a significant cause of decreasing tensile mechanical properties.

Additionally, it was shown that the thermal expansion coefficients of the reinforcing fibers (glass, flax, and jute fibers) are much smaller than that of the epoxy resin (Table 1). For example, the coefficient of thermal expansion of glass fibers is approximately 14 times less than that of epoxy resin. Furthermore, the thermal expansion coefficient is negative in the longitudinal direction of the flax fibers, but positive in the transverse direction of the flax fibers (Table 1). If a tensile specimen is heated, residual thermal stresses develop at the interface areas

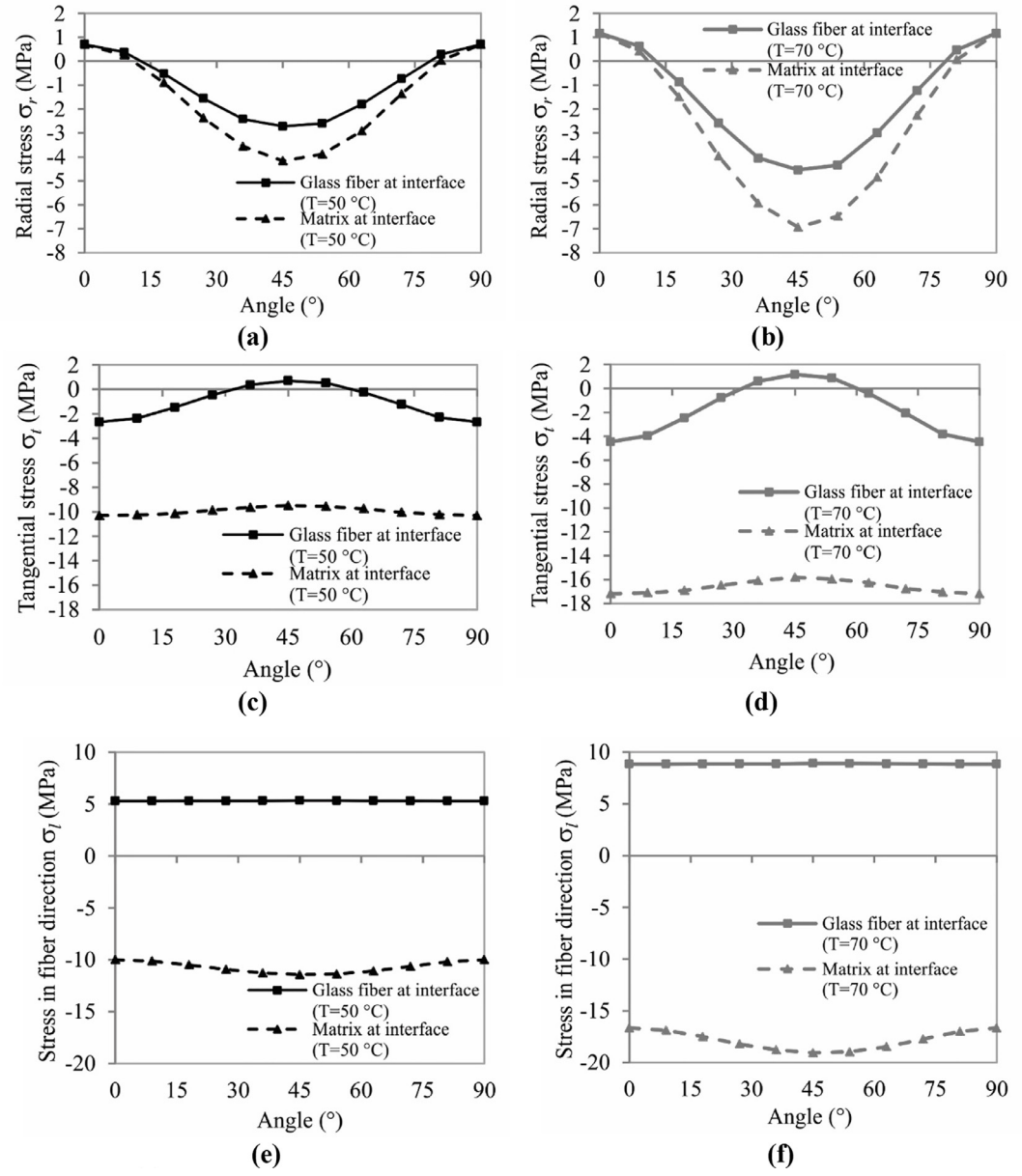

Fig. 14. Distribution of residual thermal stresses at the interface between glass fibers and the epoxy matrix after heating to $T = 50$ °C or $T = 70$ °C: (a, b) radial normal stresses σ_r, (c, d) tangential normal stressesσ_t, and (e, f) longitudinal normal stresses σ_l in the fiber direction.

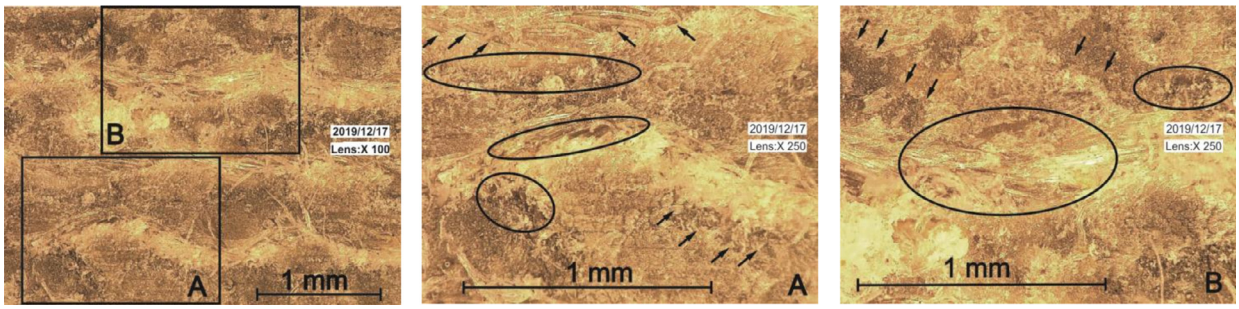

Fig. 15. Photos of damaged areas on the F-FREC composite showing micro-cracks that cause the detachment of fibers from the resin matrix after heating to 70 °C: (a) layers with marked areas A and B (lens: X 100), (b) zoomed image of area A (lens: X 250), and (c) zoomed image of area B (lens: X 250).

between the reinforcing fibers and epoxy matrix, as shown in Figs. 12 to 14. The values of the residual thermal stresses developed in fibers at the fiber-matrix interface differ from those developed in the matrix at the same points along the interface (Figs. 12 to 14) because the elastic properties and thermal expansion coefficients are different between these two components (fibers and matrix). The residual thermal stresses developed at the fiber-matrix interface are the cause of micro-cracks that lead to the detachment of fibers (flax, jute, and glass fibers) from

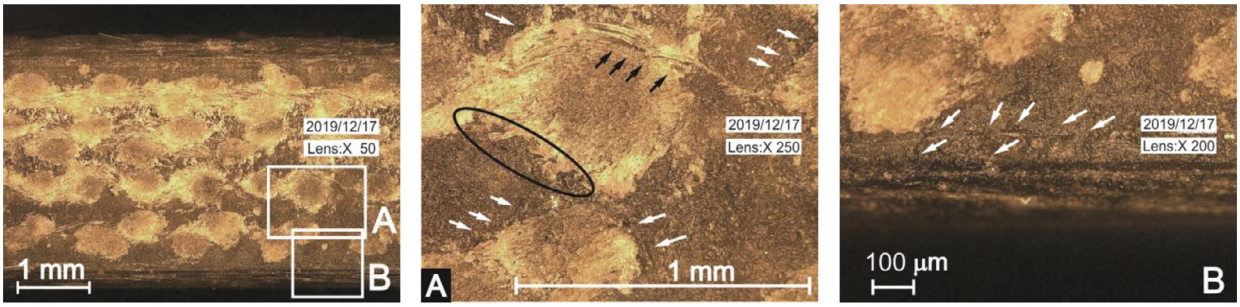

Fig. 16. Photos of damaged areas on the GF-FREC composite showing micro-cracks that cause the detachment of fibers from the resin matrix after heating to 70 °C: (a) layers with marked areas A and B (lens: X 100), (b) zoomed image of area A (lens: X 250) in a flax/epoxy layer, and (c) zoomed image of area B (lens: X 200) in a glass/epoxy layer.

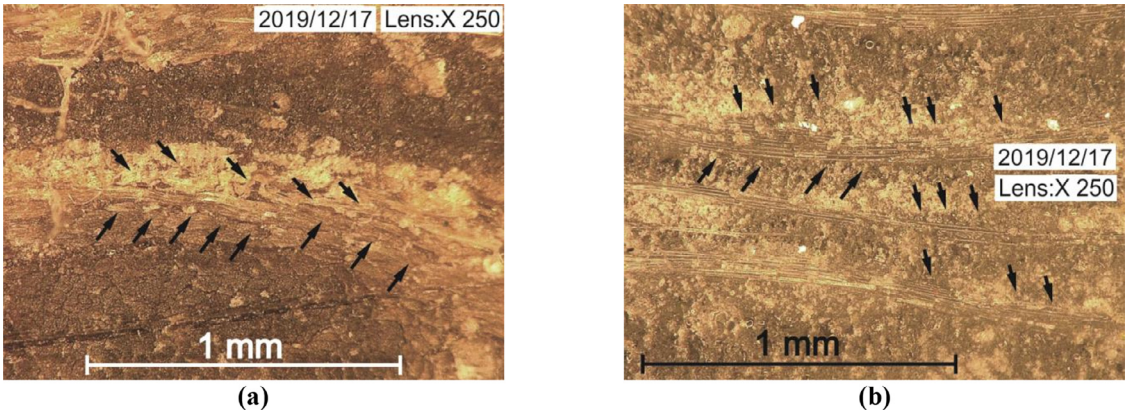

Fig. 17. Micro-cracks that cause pull-out of fibers from the matrix after heating to 70 °C: (a) J-FREC composite and (b) G-FREC composite.

the epoxy resin (Figs. 15 to 17). Resin micro-cracks caused by the heating of samples have also been reported in other studies (Aklilu et al., 2018) for polymeric composite materials reinforced with glass or carbon fibers.

Because the thermal expansion coefficient of the glass fibers is less than those of the flax and jute fibers in transverse direction of the fiber, inter-laminar micro-cracks also develop at the interfaces between layers reinforced with different materials (Fig. 16c), leading to delamination. Therefore, inter-laminar micro-cracks develop in addition to the micro-cracks developed at the interfaces between fibers and the epoxy matrix. This is why the reduction in tensile strength is the greatest for the hybrid composite materials (GF-FREC and GJ-FREC composites), as shown in Figs. 6 and 7.

5. Conclusions

This paper reported the effects of temperature changes on the tensile properties of five types of composite materials, including two hybrid composite materials whose layers were reinforced with both glass woven fabric and vegetable fibers (flax or jute fibers).

The main conclusion of our research is that the reduction in tensile strength recorded for the hybrid composite materials (GF-FREC and GJ-FREC composites) is two or three times greater than that recorded for the composite materials reinforced with only one type of fiber (F-FREC, J-FREC, and G-FREC composites).

Significant decreases in both the tensile strength and modulus of elasticity were observed for the heated specimens compared to the control specimens tested at room temperature (20 °C). These decreases are attributed to micro-cracks that develop in the epoxy matrix and at the interface between fibers and the epoxy matrix. The development of micro-cracks during specimen heating is a consequence of the different expansion coefficients of the epoxy resin used as a matrix and the reinforcing fibers (glass, flax, and jute fibers). Micro-cracks at fiber-matrix interfaces are caused by residual thermal stresses that differ between the fibers and epoxy resin for all types of reinforcement fibers, as shown in Figs. 12 to 14.

The data reported in this work are useful for the finite element analysis of parts fabricated from composite materials that are mechanically loaded with a simultaneous increase in temperature. The decreasing modulus of elasticity values of the composites highlighted in this research must be considering when defining the properties corresponding to each layer of a composite. Decreasing tensile strength should be also considered when the strength of composite structures under the effects of heating is evaluated.

Declaration of Competing Interest

The authors declare that they have no known competing financial interests or personal relationships that could have appeared to influence the work reported in this paper.

Acknowledgments

Support from the Tianjin Natural Science Foundation (No. 18JCYBJC96200) and National Natural Science Foundation of China (Grant No. 11002100) is greatly acknowledged. The authors also acknowledge the Structural Funds Project PRO-DD (POS-CCE, O.2.2.1., ID 123, SMIS 2637, ctr. No 11/2009) and Transilvania University of Brasov for providing the materials used in the manufacturing of

composites. CERBU Camelia and BOTIS Marius Florin appreciate financial support from the Tianjin University of Commerce under the framework of the Tianjin Fellowship for Foreign Visiting Professors. WANG Huaiwen appreciates financial support from the Transilvania University of Braşov under the framework of the Transilvania Fellowship for Visiting Professors.

References

Aklilu, G., Adali, S., Bright, G., 2018. Temperature effect on mechanical properties of carbon, glass and hybrid polymer composite specimens. Int. J. Eng. Res. Afr. 39, 119–138. 10.4028/. www.scientific.net/JERA.39.119.

Al-Hajaj, Z., Sy, B.L., Bougherara, H., Zdero, R., 2019. Impact properties of a new hybrid composite material made from woven carbon fibres plus flax fibres in an epoxy matrix. Compos. Struct. 208, 346–356. https://doi.org/10.1016/j.compstruct.2018.10.033.

Cerbu, C., 2015. Modeling, testing and optimization of the structures made of composite materials reinforced with fabrics and natural fibers. Habilitation thesis. Transilvania University of Brasov, Romania.

Cerbu, C., 2015. Practical solution for improving the mechanical behaviour of the composite materials reinforced with flax woven fabric. Adv. Mech. Eng. 7 (4). https://doi.org/10.1177/1687814015582084. Article Number: 1687814015582084.

Cerbu, C., 2017. Properties of some composites materials reinforced with natural fibers. In: Proceedings of The 7th International Conference on Computational Mechanics and Virtual Engineering - COMEC 2017. Brasov, November 16–17. pp. 40–44.

Cerbu, C., Cosereanu, C., 2016. Moisture effects on the mechanical behavior of fir wood flour/glass reinforced epoxy composite. Bioresources 11, 8364–8385. https://doi.org/10.15376/biores.11.4.8364-8385.

Choi, S., Sankar, B.V., 2006. Micromechanical analysis of composite laminates at cryogenic temperatures. J. Composite Mater. 40 (12), 1077–1091. https://doi.org/10.1177/0021998305057365.

Cichocki Jr, F.R., Thomason, J.L., 2002. Thermoelastic anisotropy of a natural fiber. Compos. Sci. Technol. 62 (5), 669–678. https://doi.org/10.1016/S0266-3538(02)00011-8.

Data sheet of flax fabric Tudor; DINATEX S.R.L.: Falticeni, Suceava (Romania). Available online: http://dinatex.3x.ro/pagini/contact_dinatex.html(accessed on June 23, 2019).

EN ISO 527-4: 1997. *Plastics - Determination of Tensile Properties - Part 4: Test Conditions for Isotropic and Orthotropic Fiber-Reinforced Plastic Composites*.

Habibi, M., Laperrière, L., Hassanabadi, H.M., 2019. Effect of moisture absorption and temperature on quasi-static and fatigue behavior of nonwoven flax epoxy composite. Compos. Part B-Eng. 166, 31–40. https://doi.org/10.1016/j.compositesb.2018.11.131.

Kumar, S., Singh, R.N., 1995. Three-dimensional finite element modeling of residual thermal stresses in graphite/aluminum composites. Acta Metallurgica et Materialia 43 (6), 2417–2428. https://doi.org/10.1016/0956-7151(94)00449-8.

Laine, C., Le Grognec, P., Comas-Cardona, S., Binetruy, C., 2013. Analytical, numerical and experimental study of the bifurcation and collapse behavior of a 3D reinforced sandwich structure under through-thickness compression. Int. J. Mech. Sci. 67, 42–52. https://doi.org/10.1016/j.ijmecsci.2012.12.005. hal-01666055.

Ma, G., Yan, L., Shen, W., Zhu, D., Huang, L., Kasal, B., 2018. Effects of water, alkali solution and temperature ageing on water absorption, morphology and mechanical properties of natural FRP composites: plantbased jute vs. mineral-based basalt. Compos. Part B-Eng. 153, 398–412. https://doi.org/10.1016/j.compositesb.2018.09.015.

Pitarresi, G., Tumino, D., Mancuso, A., 2015. Thermo-mechanical behaviour of flax-fibre reinforced epoxy laminates for industrial applications. Materials 8, 7371–7388. https://doi.org/10.3390/ma8115384.

Prasob, P.A., Sasikumar, M., 2019. Viscoelastic and mechanical behaviour of reduced graphene oxide and zirconium dioxide filled jute/epoxy composites at different temperature conditions. Mater.Today Commun. 19, 252–261. https://doi.org/10.1016/j.mtcomm.2019.02.005.

Properties of E-glass fibres. Available online: https://www.azom.com/properties.aspx?ArticleID=764(accessed on May 10, 2019).

Ramesh, M.Flax, 2019. (Linum usitatissimum L.) fibre reinforced polymer composite materials: A review on preparation, properties and prospects. Progr. Mater. Sci. 102, 109–166. https://doi.org/10.1016/j.pmatsci.2018.12.004.

Ridzuan, M.J.M., Abdul Majid, M.S., Khasri, A., Basaruddin, K.S., Gibson, A.G., 2019. Effect of moisture exposure and elevated temperatures on impact response of Pennisetum purpureum/glass-reinforced epoxy (PGRE) hybrid composites. Compos. Part B-Eng. 160, 84–93. https://doi.org/10.1016/j.compositesb.2018.10.029.

Safiee, S., Akil, H.M., Mazuki, A.A.M., Ishak, Z.A.M., Bakar, A.A., 2011. Properties of pultruded jute fiber reinforced unsaturated polyester composites. Adv. Compos. Mater. 20, 231–244. https://doi.org/10.1163/092430410X547047.

Saidina, D.S., Mariatti, M., Juliewatty, J., 2007. Thermal properties and dynamic mechanical properties of ceramic fillers filled epoxy composites. Proceedings of the 23rd Scientific Conference of Microscopy Society Malaysia (SCMSM 2014). AIP Publishinghttps://doi.org/10.1063/1.4919157. AIP Conf. Proc. 1669, pp. 020019-1–020019-6, ISBN 978-0-7354-1316-0.

Sathishkumar, T.P., Satheeshkumar, S., Naveen, J., 2014. Glass fiber-reinforced polymer composites – a review. J. Reinforced Plast. Compos. 33 (13), 1258–1275. https://doi.org/10.1177/0731684414530790.

Singh, H., Singh, J.I.P., Singh, S., Dhawand, V., Tiwarie, S.Kumar, 2018. A brief review of jute fibre and its composites. Mater. Today: Proc. 5, 28427–28437. https://doi.org/10.1016/j.matpr.2018.10.129.

Technical Data Sheet of glass fabric AEROGLASS 200 g/m2 twill; Havel Composites CZ: Přáslavice (Czech Republic. Available online: https://www.havel-composites.com/en/products/glass-fabric-aeroglass-200-g-m2-twill-2-2-high-strength-2694-7851(accessed on June 23, 2019).

Technical Data Sheet, 2019. Epolam 2015 Epoxy Resin. Epolam 2014-2015-2016. Hardeners Laminating System. AXSON GmbH, Dietzenbach, Germany Available online. http://www.axson.com/sites/default/files/TDS%20-%20Epolam%202015%20System%20-%20US%20REV%2002_0.pdf (accessed on May 5.

Technical Data Sheet, 2019. Epolam 2031 Epoxy Resin. Epolam 2031-2032-2033 Hardeners. Epoxy Laminating System by Infusion. AXSON GmbH, Dietzenbach, Germany Available online. https://pdf.nauticexpo.com/pdf/axson/tooling-infusion-system-epolam-2031/20406-84218.html (accessed on May 5.

Technical Data Sheet, 2019. Epolam 2035 Epoxy Resin. Epolam 2025 Hardener. Epoxy Laminating System by Infusion. AXSON GmbH, Dietzenbach, Germany Available online: http://www.uni-trading.com/sub/support/tds.msds/resin/suji_Tooing/EPOXY%20LAMENATING%20RESINS/TOOLING/TDS/EPOLAM2035-2025-TDS(EN).pdf (accessed on May 5.

Technical data sheet, 2019. Fiberglass: Strength and Thermal Stability. FIBER-LINE® LLC, HatfieldUSA Available online: https://www.fiber-line.com/en/fibers/fiberglass (accessed on June 23.

Thomason, J., Yang, L., Gentles, F., 2017. Characterisation of the anisotropic thermoelastic properties of natural fibres for composite reinforcement. Fibers 5, 36–47. https://doi.org/10.3390/fib5040036.

Xu, D., Cerbu, C., Wang, H., Rosca, I.C., 2019. Analysis of the hybrid composite materials reinforced with natural fibers considering digital image correlation (DIC) measurements. Mech. Mater. 135, 46–56. https://doi.org/10.1016/j.mechmat.2019.05.001.

Yan, L., Chouw, N., Jayaraman, K., 2015. Effect of UV and water spraying on the mechanical properties of flax fabric reinforced polymer composites used for civil engineering applications. Mater. Des. 71, 17–25. https://doi.org/10.1016/j.matdes.2015.01.003.